PHYSICAL REVIEW B **85**, 081102(R) (2012)

Ultrafast pump-probe measurements of short small-polaron lifetimes in the mixed-valence perovskite $Cs_2Au_2I_6$ under high pressures

M. Trigo,[1,2,*] J. Chen,[1,2] M. P. Jiang,[1,2] W. L. Mao,[2,3] S. C. Riggs,[2,4] M. C. Shapiro,[2,4] I. R. Fisher,[2,4] and D. A. Reis[1,2,5]

[1]*Stanford PULSE Institute, SLAC National Accelerator Laboratory, Menlo Park, California 94025, USA*

[2]*Stanford Institute for Materials and Energy Science, SLAC National Accelerator Laboratory, 2575 Sand Hill Road, Menlo Park, CA 94025*

[3]*Department of Geological & Environmental Sciences, Stanford University, Stanford, California 94305, USA*

[4]*Department of Applied Physics and Geballe Laboratory for Advanced Materials, Stanford University, Stanford, California 94305, USA*

[5]*Department of Photon Science and Applied Physics, Stanford University, Stanford, California 94305, USA*

(Received 28 December 2011; published 3 February 2012)

We study the ultrafast phonon response of mixed-valence perovskite $Cs_2Au_2I_6$ using pump-probe spectroscopy under high pressure in a diamond-anvil cell. We observed a remarkable softening and broadening of the Au-I stretching phonon mode with both applied pressure and photoexcitation. Using a double-pump scheme we measured a lifetime of the charge-transfer excitation into single-valence Au^{2+} of less than 4 ps, which is an indication of the local character of the Au^{2+} excitation. Furthermore, the strong similarity between the pressure and fluence dependence of the phonon softening shows that the intervalence charge transfer plays an important role in the structural transition.

DOI: 10.1103/PhysRevB.85.081102 PACS number(s): 78.47.J−, 78.20.hb

Mixed-valence (MV) materials based on $4f$ elements have historically attracted considerable attention.[1,2] In materials such as the samarium chalcogenides as well as in many cerium intermetallic compounds, the valence fluctuates rapidly between f^n and f^{n-1}, but the average valence is nevertheless homogeneous.[3,4] Driven by hybridization with itinerant carriers, this behavior is intimately related to the Kondo effect.[5] A distinctly different type of mixed valence occurs for some d-block elements for which Jahn-Teller effects stabilize static (inhomogeneous) d^{n-1} and d^{n+1} configurations.[1] Much less is known about valence fluctuations in this class of material, for which coupling to the crystal lattice clearly plays an important role. Here we study $Cs_2Au_2I_6$, which is a canonical example of a $5d$ mixed-valence system exhibiting charge disproportionation.[6] Of particular interest, this material undergoes a first-order coupled structural and valence transition at a moderately low pressure of just 5.5 GPa.[7,8] Using ultrafast pump-probe spectroscopy we make a quantitative comparison of the effects of photoinduced valence transitions with those of hydrostatic pressure, as revealed by softening of the phonon spectra. The clear similarity between these two cases confirms that the structural transition is associated with the intervalence charge transfer (IVCT) between the distinct Au sites. The photoinduced state has a remarkably short lifetime, indicative of local (small) polaronic excitations rather than extended states.

The $Cs_2Au_2X_6$ family, with X = Cl, Br, or I, is a mixed-valence perovskite that shows a pressure-induced phase transition at 11, 9, and 5.5 GPa as the size of the halogen atom increases from Cl, to Br, and to I, respectively.[6,9,10] In the low-pressure phase, the gold ion appears in a MV state with alternating Au^{1+} and Au^{3+} sites, and the surrounding halogen ions form a distorted octahedron as depicted in Fig. 1(a). At the critical pressure the system transforms from MV to single valent (SV) and all the Au ions acquire a valence 2+.[11] At this point the surrounding halogen ions shift to the symmetric position between neighboring Au^{2+} [Fig. 1(a)] and the associated lattice distortion disappears.[6] As in the insulator $BaBiO_3$, the strong coupling between the charge disproportionation of the metal ion and the lattice deformation stabilizes the commensurate charge-density wave (CDW).

Pump-probe experiments were performed using pulses from a Ti:sapphire regenerative amplifier laser (Coherent Rega) with a nominal pulse duration of 50 fs and a central wavelength of 800 nm. After the amplifier, 50% of the beam was split to seed an optical parametric amplifier (OPA) which provides pulses with ∼0.12 μJ of energy at a central wavelength of 550 nm. The other 50% of the beam was split into probe (800 nm) and pump (400 nm) which was frequency doubled on a nonlinear beta barium borate (BBO) crystal [see Fig. 1(b) for a diagram of the three-pulse sequence used later in the text]. Depending on the configuration of the experiment (see the discussion below), a combination of pulses with wavelengths 800, 550, and 400 nm were overlapped to a spot ∼10 μm in diameter inside a diamond-anvil cell (DAC) with a microscope objective [see Fig. 1(b)]. The backscattered light was refocused and spatially filtered with a 100-μm pinhole, which was then imaged onto a Si photodiode. A color filter in front of the detector rejected scattered 400-nm pump light. The 400-nm pump was chopped at 1.6 kHz and a lock-in scheme was used to detect the differential reflectivity at 800 nm. The probe fluence was kept below 0.3 mJ/cm^2. Single crystals of $Cs_2Au_2I_6$ were prepared by a self-flux technique, as described elsewhere.[12] Samples were crushed in the DAC in order to ensure that backscattered light reached the detector. The gasket hole was 200 μm in diameter and silicone oil was used as the pressure medium. The pressure was calibrated by monitoring the fluorescence of a small ruby crystal inside the DAC.

Figure 2 shows pump (400 nm)-probe (800 nm) traces for varying pressure [Fig. 2(a)] and their Fourier transforms [Fig. 2(b)]. Curves in Fig. 2(a) were filtered by subtracting a moving average to remove the slowly varying background. All the traces were taken with the same pump fluence ∼0.3 mJ/cm^2, which is low enough to avoid softening the phonon mode significantly by photoexcitation. At the lowest pressure, the phonon oscillations appear close to 3.7 THz, as seen in the Fourier transform [Fig. 2(b), lowest trace].

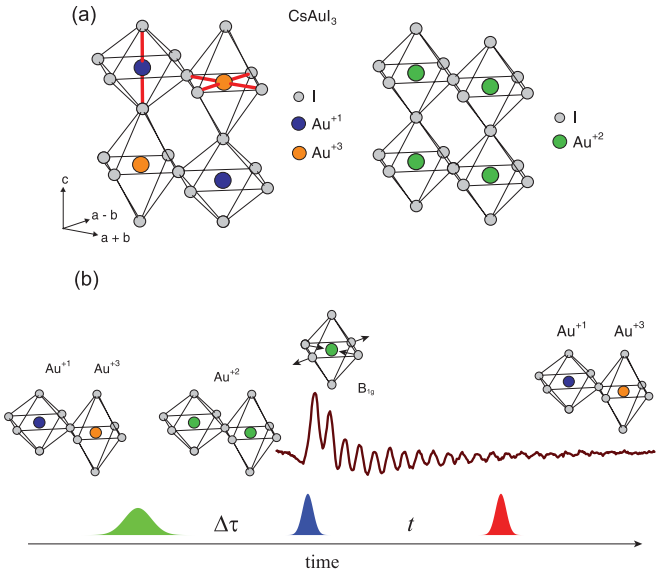

FIG. 1. (Color online) (a) The structure of $Cs_2Au_2I_6$ in the mixed-valence (left) and single-valence (right) states with the accompanying band Jahn-Teller lattice distortion [for clarity, the Cs atoms are not displayed]. (b) Schematic diagram of the three pulse scheme for high-pressure pump-probe spectroscopy discussed in the text: A stretched pulse (left) induces the IVCT $Au^{1+} \rightarrow Au^{3+}$, a delayed short pulse (center) excites coherent modes, and a third pulse (right) probes the reflectivity changes due to the phonon.

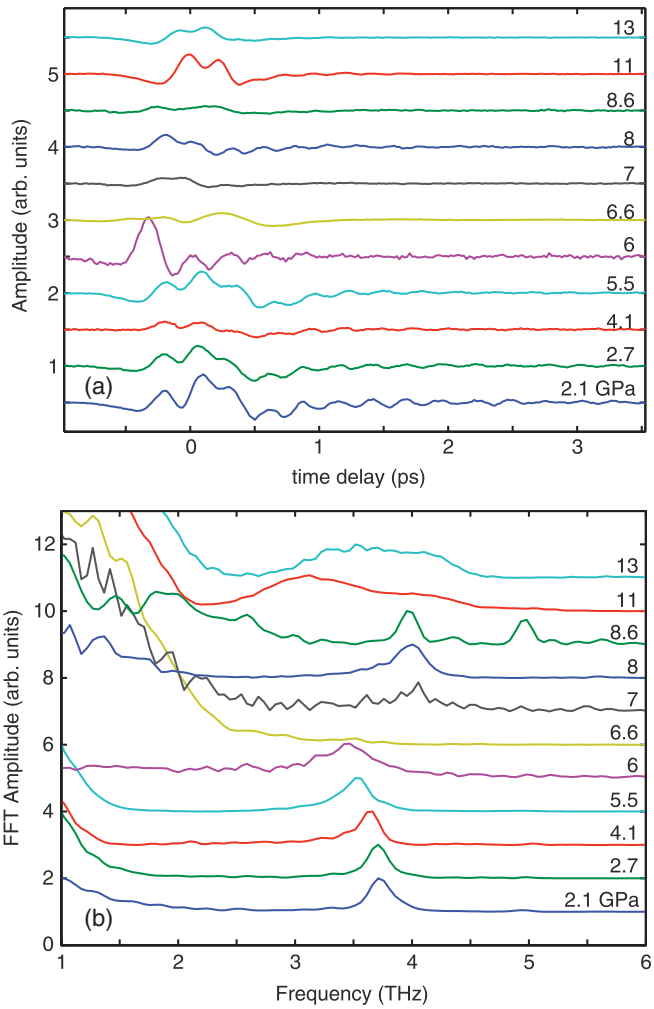

FIG. 2. (Color online) (a) Oscillatory component of the differential reflectivity for different hydrostatic pressures (listed to the right of each trace). (b) Fourier transforms of the traces in (a). The phonon mode near 3.6 THz disappears at ∼6.6 GPa and oscillations with a frequency of 4 THz appear above the transition around 8 GPa.

This oscillation is assigned to the B_{1g} stretching mode of the distorted I_6 octahedron surrounding the Au atoms. The displacement associated with this mode is schematically drawn in Fig. 1(b). As pressure approaches the phase transition near 6 GPa, the frequency softens and the peak broadens and eventually disappears at ∼6.6 GPa [Fig. 2(b)]. Similar softening behavior due to the freezing of the Jahn-Teller-like modes has been observed at room temperature in the Raman spectra of $Cs_2Au_2Br_6$ and $Cs_2Au_2Cl_6$ at 9 and 11 GPa, respectively.[9] The Raman intensity of the B_{1g} mode vanishes above the transition due to the doubling of the Brillouin zone, which unfolds the zone-center B_{1g} mode into the edge of the new Brillouin zone, making this mode inaccessible to Raman scattering due to its large wave vector.[13] Above the transition ($P > 7$ GPa), different oscillations appear at >4 THz, which must originate from different zone-center modes of the high-pressure phase. Eventually these oscillations also disappear above ∼13 GPa, where the material may become amorphous.[14]

Many of the physical properties of $Cs_2Au_2I_6$ can be understood by thinking of the system as being composed of alternating linear $[Au^{1+}I_2]^-$ and square planar $[Au^{3+}I_4]^-$ molecules,[8] as represented by the nearest-neighbor bonds in Fig. 1(a). The observed oscillations can be ascribed to the coherent motion of the B_{1g} mode of the square $[Au^{3+}I_4]^-$ molecule.[6] At ambient pressure we observed a weak peak at 4.6 THz that we assign to the higher-frequency A_{1g} mode of the linear $[Au^{1+}I_2]^-$molecule. However, this mode vanishes at lower pressure than the B_{1g} mode[9] and was not visible at $P > 2$ GPa. At 3.5 GPa, $Cs_2Au_2I_6$ is in the mixed-valence state with alternating Au^{1+} and Au^{3+} cations [Fig. 1(a)]. As the pressure increases above ∼5.5 GPa, increased overlap between the molecular orbitals of the gold iodide complexes is thought to drive the system into the single Au^{2+} valence. The suppression of the Au^{1+}-Au^{3+} charge order relaxes the octahedral distortion,[6,10] and results in the softening and broadening of the phonon mode as seen in Fig. 2(b). Significantly, the IVCT between the 5*d* orbitals can also be achieved by photoexcitation in the visible region of the spectrum.[6] As we show next, photoexcitation has a similar effect on the phonon response as pressure, and argue that there is a direct analogy between the effect of pressure and photoexcitation on the system since both induce the IVCT.

Figure 3(a) shows single pump (400 nm)-probe (800 nm) differential reflectivity traces at ∼3.5 GPa for increasing pump fluences. The traces were normalized to their maximum value for displaying purposes (however, their amplitude is linear with fluence). Figure 3(a) shows coherent oscillations similar to those in Fig. 2, which correspond to the same B_{1g} stretching mode of the I_6 octahedron sketched in Fig. 1(a). The oscillation in the lowest fluence trace in Fig. 3(a) (top trace) shows a slight frequency chirp that starts at 3.61 THz

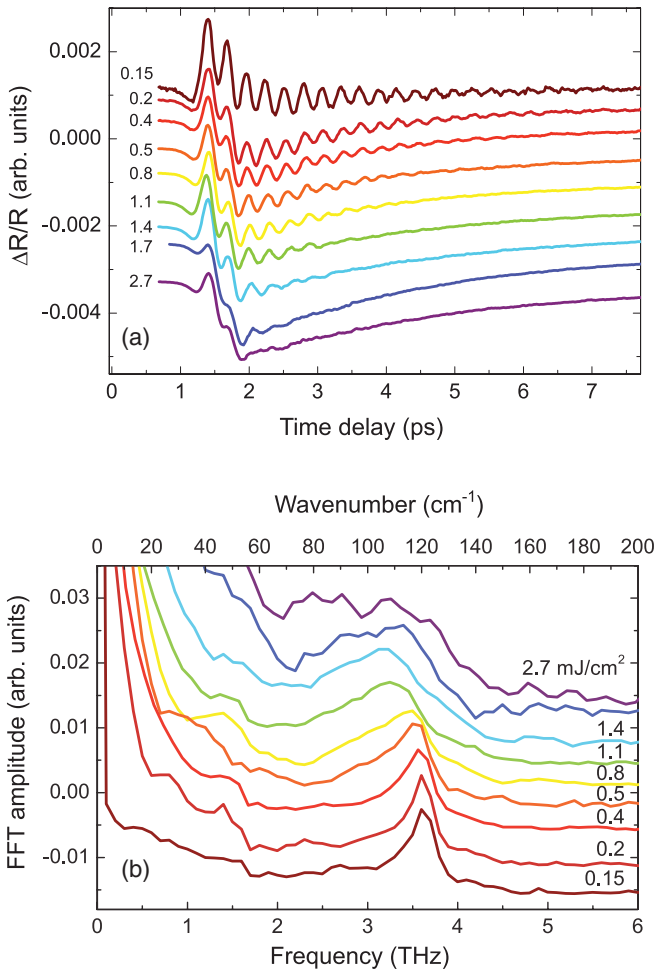

FIG. 3. (Color online) (a) Time dependence of the differential reflectivity for different 400-nm pump fluences at 3.5 GPa. The traces are normalized by their maximum amplitude for clarity. Incident fluences in mJ/cm^2 are shown next to each trace. (b) Representative Fourier transforms of time traces for different pump fluences (normalized).

(277-fs period) measured at the first oscillation cycle that becomes 3.74 THz (267-fs period) at the sixth cycle. The softening induced by the absorption of the pump pulse is more evident in the Fourier transforms of these traces as shown in Fig. 3(b), where the peak at ∼3.6 THz softens and broadens as the pump fluence is increased. At higher excitations the phonon oscillation was less visible due to the quickly decaying phonon amplitude and the large background. Note that the maximum fluence 2.7 mJ/cm^2 corresponds to $\sim 5 \times 10^{15}$ photons/cm^2, well below the nucleation threshold for complete transformation to single valence reported for $Cs_2Au_2Br_6$.[15] The picture that emerges from the pressure and fluence dependence in Figs. 2 and 3 is the following: As pressure increases, a gradual overlap between the $5d_{x^2-y^2}$ orbitals of Au^{1+} and Au^{3+} due to the crystal-field modification induces the transition to the single-valence Au^{2+} at 5.5 GPa.[6] In a completely analogous way, optical excitation induces the IVCT $Au^{1+} \rightarrow Au^{3+}$ suppressing the charge modulation, which results in a softening and deactivation of the phonon. In this discussion, the short pump pulse plays two roles: It excites the coherent B_{1g} motion impulsively,[16] which leads to the modulation of the optical reflectivity in Fig. 3(a), and at the same time produces the IVCT $Au^{1+} \rightarrow Au^{3+}$, which induces the observed softening of the phonon mode.

In order to gain a better understanding of the photoexcited state it is useful to separate the optical IVCT from the impulsive excitation of the phonon. To do this, we implemented a three-pulse pump-probe scheme depicted schematically in Fig. 1(b): The first pulse induces the electronic charge transfer (left, 550 nm). This photon energy is close to the $5d_{xy} \rightarrow 5d_{x^2-y^2}$ transition between Au^{1+} and Au^{3+},[17] which "prepares" the system into a significant fraction of Au^{2+} sites. The pulse duration was stretched to 600 fs to avoid generating coherent phonons by impulsive excitation[16] with the "preparation" pulse. A delayed short pulse (center, 400 nm) impulsively excites the coherent motion of the phonon of the IVCT state, which is softened by the photoinduced homogeneous charge distribution. Finally, a third weak pulse (right, 800 nm) with a different optical delay probes the differential optical reflectivity. We define $\Delta\tau$ as the delay between the IVCT pulse (550 nm) and the phonon pump (400 nm), while "probe delay" is the usual delay between the coherent phonon pump (400 nm) and the probe pulse (800 nm). In this way, with independent control of the delays we measure the impulsive phonon response of the intermediate state and use it as a probe of the dynamics of the IVCT excitation.

Figure 4(a) shows time-resolved differential reflectivity versus probe delay for different $\Delta\tau$. The traces resemble the single-pump data in Fig. 3(a) with coherent oscillations due to the B_{1g} phonon mode around 3.7 THz. However, here each curve represents the phonon response to an impulsive force at time $\Delta\tau$ after the IVCT "preparation" pulse (i.e., $\Delta\tau$ after creation of Au^{2+} sites). As with the fluence data in Fig. 3, the oscillations are softened and strongly damped, particularly for small $\Delta\tau$, i.e., immediately after the IVCT excitation [top trace in Fig. 4(a)]. As $\Delta\tau$ increases [Fig. 4(a), top to bottom] the IVCT relaxes back to equilibrium and the phonon response recovers toward the single-pump trace labeled "no IVCT." The 400-nm fluence was kept low to avoid additional softening of the mode. Figure 4(b) shows the frequency and decay constant of the oscillations in Fig. 4(a) versus $\Delta\tau$ extracted by fitting the oscillatory component of the time trace with a decaying cosine function. For comparison, Figs. 4(c) and 4(d) show the fluence and pressure dependence of these parameters from the data in Figs. 2 and 3 [on the same scale as in Fig. 4(b)]. Figure 4(b) brings out more clearly the softening due to the IVCT: The frequency (black squares) drops to almost 85% of the nominal value near $\Delta\tau = 0$ while at $\Delta\tau \sim 4$ ps it has already recovered to >97% of the value for the unperturbed phonon (open symbols). This represents a measurement of the lifetime of the IVCT excitation. Such a fast recovery time for the charge is unusual for typical extended states in solids which can range up to μs in some semiconductors, and is likely due to the local nature of the charge excitation associated with the induced Au^{2+} small-polaron sites.[14] The decay constant also varies drastically with $\Delta\tau$, fluence, and pressure [triangles in Figs. 4(b)–4(d)]. This behavior can be explained by an inhomogeneous broadening caused by the presence of single- and mixed-valence clusters of varying

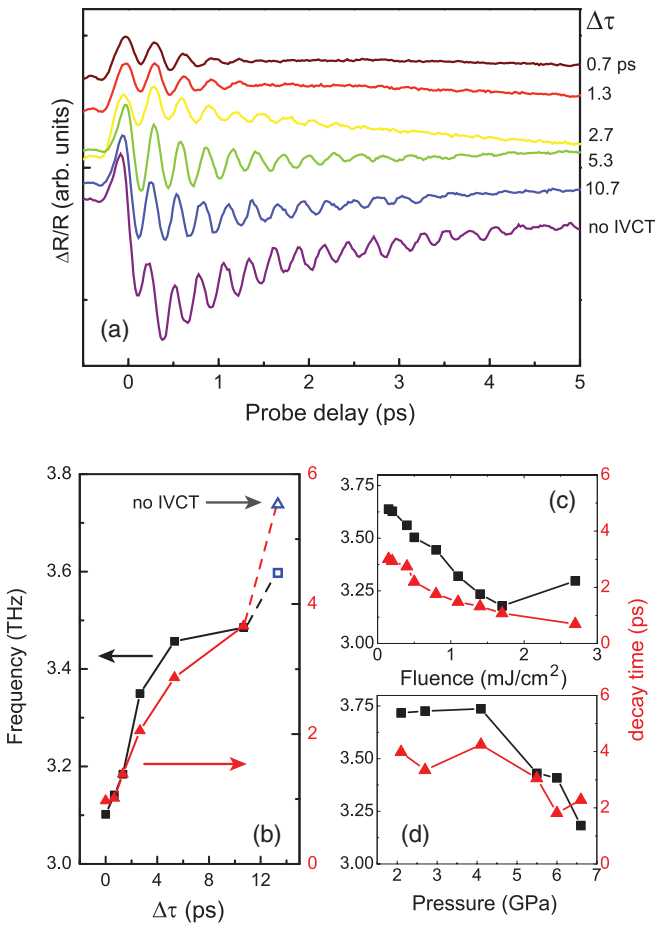

FIG. 4. (Color online) (a) Coherent phonon response at 3.5 GPa for different delays $\Delta\tau$ after charge-transfer excitation with 550-nm pulses. (b) Frequency and decay constant of the coherent oscillations in (a) as a function of charge transfer pump delay $\Delta\tau$. (c) Fluence and (d) pressure dependence of the frequency and decay constant of the oscillations from Figs. 2 and 3.

sizes.[18] Indeed, a Gaussian distribution of decaying oscillators with variance $\sigma = 0.5$ THz gives $\tau_{1/e} = 2.2$ ps, assuming an intrinsic oscillator linewidth of $\Gamma = 1/6$ (ps^{-1}) (estimated from the decay of the unperturbed "no IVCT" trace). These values are consistent with the range of decay times observed in Figs. 4(b)–4(d), indicating that the decay in the signal is mostly due to inhomogeneous broadening. Note, however, that we cannot rule out a contribution to the broadening due to inhomogeneous pump illumination. Finally, the similarity between the pressure and fluence dependence in Figs. 4(c) and 4(d) is consistent with a picture in which the phonon softening and thus the structural transition is intimately connected with the charge-transfer excitation.

In conclusion, we studied the ultrafast phonon response of $Cs_2Au_2I_6$ *in situ* using pump-probe spectroscopy under high pressure inside a DAC. We observed a remarkable softening and broadening of the B_{1g} Au-I stretching phonon mode with both applied pressure and photoexcitation. This mode involves motion of the distorted I_6 octahedron surrounding the Au ion, and thus is strongly coupled with the Au valence electrons. We observe a strong similarity between the pressure and fluence dependence of the phonon response, which is consistent with a picture in which the IVCT and the structural transition are intimately connected. Furthermore, using a three-pulse pump-probe sequence we measured a lifetime of the IVCT excitation of <4 ps. We argue that such a fast recovery of the valence is an indication of the local (small-polaron) character of the Au^{2+} excitation, which also provides compelling evidence for the system being nonmetallic. These results also demonstrate the utility of pump-probe spectroscopy to probe the dynamics of excitations in correlated matter under high pressure.

ACKNOWLEDGMENTS

M.T., J.C., M.P.J., W.L.M. and D.R. acknowledge support from the US Department of Energy office of Basic Energy Science through the Division of Materials Sciences and Engineering under contract DE-AC02-76SF00515. S.C.R., M.S. and I.R.F. are supported by the AFOSR Grant No. FA9550-09-1-0583. We would like to thank Yu Lin for experimental assistance.

*mtrigo@slac.stanford.edu

[1] M. B. Robin and P. Day, *Mixed Valence Chemistry-A Survey and Classification* (Academic, New York, 1968).
[2] C. M. Varma, Rev. Mod. Phys. **48**, 219 (1976).
[3] J. M. D. Coey, S. K. Ghatak, M. Avignon, and F. Holtzberg, Phys. Rev. B **14**, 3744 (1976).
[4] E. Annese, A. Barla, C. Dallera, G. Lapertot, J.-P. Sanchez, and G. Vankó, Phys. Rev. B **73**, 140409 (2006).
[5] A. C. Hewson, *The Kondo Problem to Heavy Fermions* (Cambridge University Press, Cambridge, UK, 1997).
[6] N. Kojima, Bull. Chem. Soc. Jpn. **73**, 1445 (2000).
[7] N. Kojima, M. Hasegawa, H. Kitagawa, T. Kikegawa, and O. Shimomura, J. Am. Chem. Soc. **116**, 11368 (1994).
[8] N. Matsushita, H. Kitagawa, and N. Kojima, Acta Crystallogr. Sect. C **53**, 663 (1997).
[9] X. J. Liu, Y. Moritomo, A. Nakamura, and N. Kojima, J. Chem. Phys. **110**, 9174 (1999a).
[10] N. Matsushita, H. Ahsbahs, S. S. Hafner, and N. Kojima, J. Solid State Chem. **180**, 1353 (2007).
[11] S. Hafner, N. Kojima, J. Stanek, and L. Zhang, Phys. Lett. A **192**, 385 (1994).
[12] S. C. Riggs, M. C. Shapiro, F. Corredor, T. H. Geballe, I. R. Fisher, G. T. McCandless, and J. Y. Chan, e-print arXiv:1111.7017v1.
[13] R. Loudon, Adv. Phys. **50**, 813 (2001).
[14] A. F. Kusmartseva, M. Yang, A. M. Arevalo-Lopez, K. V. Kamenev, and J. P. Attfield, Chem. Commun. **46**, 6681 (2010).
[15] X. J. Liu, Y. Moritomo, M. Ichida, A. Nakamura, and N. Kojima, Phys. Rev. B **61**, 20 (2000a).
[16] R. Merlin, Solid State Commun. **102**, 207 (1997).
[17] X. J. Liu, K. Matsuda, Y. Moritomo, A. Nakamura, and N. Kojima, Phys. Rev. B **59**, 7925 (1999b).
[18] X. Liu, Y. Moritomo, M. Ichida, A. Nakamura, and N. Kojima, J. Phys. Soc. Jpn. **69**, 1267 (2000b).